# Travel time approach to kinetically sorbing solute by diverging radial flows through heterogeneous porous formations

Gerardo Severino,[1] Samuele De Bartolo,[2] Gerardo Toraldo,[1,3,4] Gowri Srinivasan,[5] and Hari Viswanathan[5]

Received 29 June 2012; revised 16 October 2012; accepted 2 November 2012; published 21 December 2012.

[1] Diverging radial flow takes place in a heterogeneous porous medium where the log conductivity $Y = \ln K$ is modeled as a stationary random space function (RSF). The flow is steady, and is generated by a fully penetrating well. A linearly sorbing solute is injected through the well envelope, and we aim at computing the average flux concentration (*breakthrough curve*). A relatively simple solution for this difficult problem is achieved by adopting, similar to Indelman and Dagan (1999), a few simplifying assumptions: (i) a thick aquifer of large horizontal extent, (ii) mildly heterogeneous medium, (iii) strongly anisotropic formation, and (iv) large Peclet number. By introducing an appropriate Lagrangian framework, three-dimensional transport is mapped onto a one-dimensional domain ($\tau$, $t$) where $\tau$ and $t$ represent the fluid travel and current time, respectively. Central for this approach is the probability density function of the RSF $\tau$ that is derived consistently with the adopted assumptions stated above. Based on this, it is shown that the travel time can be regarded as a Gaussian random variable only in the far field. The breakthrough curves are analyzed to assess the impact of the hydraulic as well as reactive parameters. Finally, the travel time approach is tested against a forced-gradient transport experiment and shows good agreement.

**Citation:** Severino, G., S. De Bartolo, G. Toraldo, G. Srinivasan, and H. Viswanathan (2012), Travel time approach to kinetically sorbing solute by diverging radial flows through heterogeneous porous formations, *Water Resour. Res.*, *48*, W12527, doi:10.1029/2012WR012608.

## 1. Introduction

[2] Transport tracer tests at aquifer scale represent a powerful tool to estimate formation parameters (a general overview can be found in *Ptak et al.* [2004]). In fact, since under natural gradient conditions the flow velocity is generally small, it is a common practice to force the flow by using injecting/pumping wells. Another typical application of the well-flow is provided by the *pump* and *treat* procedure to extract pollutants from the groundwater. Therefore, it is of definite interest to model transport determined by well flow (WF). Although transport in a radial configuration largely differs from transport under natural gradient conditions, also referred hereafter as transport in mean uniform (MU) flows, parameters estimated from either the first or the second case are often compared without distinction [*Gelhar et al.*, 1992]. In particular, large differences are observed if one uses the MU configuration to identify the hydraulic properties of an aquifer where the flow pattern is clearly radial [*Fernandez-Garcia et al.*, 2004]. Only recently theoretical studies [e.g., *Indelman et al.*, 1996; *Fiori et al.*, 1998; *Guadagnini et al.*, 2003; *Severino et al.*, 2008] on radial flows in three-dimensional heterogeneous porous formations have been undertaken with the aim to support practical applications [e.g., *Dagan and Indelman*, 1999; *Lessoff and Indelman*, 2004; *Indelman et al.*, 2006; *Severino et al.*, 2011].

[3] We consider here steady flow determined by a fully penetrating well charging at constant specific (per unit depth) volumetric rate $Q_w$ and given head $H_w$. The aquifer $\Omega$ is horizontally unbounded with thickness $B$ (Figure 1). A solute is injected within the aquifer through the well screen, and the solute concentration is monitored by means of a battery of recovering wells at the same radial distance $r$ from the release zone. The simple case of a homogeneous formation was investigated in the past by accounting for advection and pore-scale dispersion [*Hsieh*, 1986; *Chen*, 1987]. These results mainly apply at laboratory scale [*Dagan*, 1986]. At aquifer scale, the solute spreading is primarily dominated by the spatial variability of the advective mechanism [*Valocchi*, 1986], so that it is customary to neglect the impact of pore-scale dispersion (large Peclet-number regime). The first analytical study of transport in a radially diverging

[1]Water Resources Management and Bio System Engineering, University of Naples "Federico II," Portici, Naples, Italy.
[2]Department of Civil Engineering, University of Calabria, Rende, Cosenza, Italy.
[3]Department of Mathematics and Applications "R. Caccioppoli," Università degli Studi Napoli "Federico II," Naples, Italy.
[4]Also at Water Resources Management and Bio System Engineering, University of Naples "Federico II," Portici, Naples, Italy.
[5]Theoretical Division, Los Alamos National Laboratory, Los Alamos, New Mexico, USA.

Corresponding author: G. Severino, Water Resources Management and Bio System Engineering, University of Naples "Federico II," Portici, I-80055 Naples, Italy. (gerardo.severino@unina.it)


0043-1397/12/2012WR012608

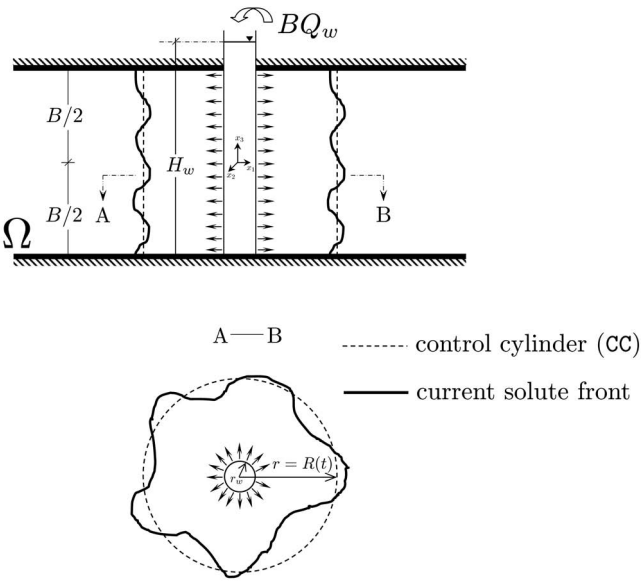


**Figure 1.** Realization of solute spreading by a diverging radial flow.

flow is from *Indelman and Dagan* [1999]. This study has also inspired the analysis of transport in converging flows [see, e.g., *Dagan and Indelman*, 1999; *Lessoff and Indelman*, 2004; *Riva et al.*, 2006; *Indelman et al.*, 2006]. However, the dispersion mechanism in transport by converging flows significantly differs from that of diverging flows. To illustrate the implications upon the spreading mechanism, let us consider the simplest case of a homogeneous medium (i.e., heterogeneity is not accounted for) and assume that the pore-scale dispersion can be neglected. In a converging flow, due to the axial symmetry of the steady flow, solute particles released at a given radial distance will take the same time to reach the well. By using a similar kinematical picture for diverging flows, any particle released at the well will take the same time to reach the control cylinder (CC; irrespective of the polar angle).

[4] In a heterogeneous medium, the spreading mechanism is mainly determined by the fluctuations of the macroscopic velocity that are caused in turn by the spatial variability of the conductivity. As a consequence, solute particles that experience highly conducting inclusions will reach the well sooner and vice versa. This large effect is enhanced by the nonuniformity of the flow, resulting in huge differences in travel time (in both converging and diverging flows). The overall effect is that the breakthrough curve (BTC) determined by a solute pulse will display a bell-shaped distribution. However, in the case of transport in radially diverging flows, the characterizing feature (that is not detected in transport in converging flows) is the large distance behavior, where the macrodispersivity is constant [*Indelman* and *Dagan*, 1999] similar to what is observed in MU flows. This is explained by recalling that far away from the well, the flow (and concurrently transport) behaves as a MU one [see, e.g., *Severino et al.*, 2008].

[5] A useful characterization of transport in aquifers can be formulated in terms of average flux concentration [e.g., *Dagan et al.*, 1992; *Cvetkovic and Dagan*, 1994] since it is consistent with common procedures for measuring concentrations [e.g., *Andricevic and Cvetkovic*, 1997]. The average flux concentration was considered in numerous studies dealing with MU flows [e.g., *Cvetkovic and Dagan*, 1994; *Cvetkovic et al.*, 1998; *Severino et al.*, 2012]. Current regulatory standards for the subsurface environment, especially those set in terms of the *travel time approach*, make the solute flux approach an appealing framework for predicting/analyzing subsurface contaminant transport. The travel time approach to model solute transport by radial flows in three-dimensional heterogeneous porous formations has been considered in both a conditional [e.g., *Sanchez-Vila and Rubin*, 2003] and unconditional [e.g., *Indelman et al.*, 2006] framework.

[6] We consider an injection of a solute in the aquifer, and we aim to determine the average flux concentration $\overline{C}^f$ at any radial distance from the well related to the heterogeneity of the conductivity $K$ (Figure 1). For a fully penetrating well of length $B \gg I_v$, the ergodic hypothesis may be invoked, i.e., $\overline{C}^f \simeq \langle C^f \rangle$ (being here and in the following $\langle\rangle$ the ensemble average operator). Thus, we consider the mean concentration as obtained by ensemble averaging the recovered effluent curves from monitoring wells located at the same radial distance. Such a concentration is also termed as BTC. To compute this latter, we shall adapt the procedure that was formulated by *Cvetkovic and Dagan* [1994] for MU flows, and subsequently modified by *Dagan and Indelman* [1999] for the so-called doublet problem. To achieve a simple solution for the flow field, we make use of the approximate solution obtained by *Indelman and Dagan* [1999]. We have shown, unlike previous studies, that the assumption of normality in the travel time distribution is valid only in the far field. Then, we derive and discuss BTCs pertaining to both conservative and reactive solutes. Finally, the proposed approach is tested against a transport experiment to demonstrate the usefulness of this stochastic method for interrogating forced-gradient tests.

## 2. Problem Statement

### 2.1. Flow Configuration

[7] We deal with an aquifer of constant thickness $B$ and unbounded horizontal extent. Due to its erratic spatial variability, the hydraulic conductivity $K$ cannot be measured and mapped accurately. Thus, we regard it as a random space function (RSF), and assume that $Y = \ln K$ is stationary and normal, defined completely by its ensemble mean $\langle Y \rangle$, its variance $\sigma_Y^2$, and the two-point autocorrelation $\rho_Y$. This latter is modeled as anisotropic, with the horizontal integral scale $I$ larger than the vertical one $I_v$ [see, e.g., *Rubin*, 2003].

[8] A fully penetrating well of radius $r_w$ is injecting at given volumetric rate $BQ_w$ (where $Q_w$ the volumetric rate per unit depth). The head $H$ along the well water column is constant, i.e., $H = H_w$ for $r = r_w$ (Figure 1), whereas in the flow domain, it satisfies the equation

$$\nabla \cdot (K \nabla H) = 0 \quad \text{in} \quad \Omega = \{\mathbf{x} \equiv (x_1, x_2, x_3) : r = \sqrt{x_1^2 + x_2^2} \geq r_w,\ -B/2 \leq x_3 \leq B/2\}. \tag{1}$$

[9] The mass conservation at the well (written in cylindrical coordinates) requires that

$$\frac{r_w}{B}\int_{-B/2}^{B/2}\int_0^{2\pi} \mathrm{d}x_3\,\mathrm{d}\theta\, q_0(r_w, x_3, \theta) = Q_w, \tag{2}$$

where $q_0$ is the radial component of the specific discharge at the well envelope. The solution of the flow field yields the head $H$ and specific discharge $\mathbf{q} = -\exp(Y)\nabla H$ as functions of $Y$.

### 2.2. Transport Problem

[10] Let $C$ be the solute concentration (mass of solute per volume of fluid). With the neglect of pore-scale dispersion (large Peclet number), $C$ satisfies the reactive advective transport equation

$$\frac{\partial}{\partial t}(C+N) + V_i(\mathbf{x})\frac{\partial}{\partial x_i}C = 0, \qquad \mathbf{V} = \frac{\mathbf{q}}{n} \equiv (V_1, V_2, V_3), \tag{3}$$

where $N$ is the concentration sorbed on the matrix of the medium (mass of sorbed solute per volume of fluid). The transport equation (3) is solved for a generic boundary condition, whereas the medium is assumed to be initially solute-free, i.e., $C(\mathbf{x}, 0) = N(\mathbf{x}, 0) = 0$. Several physical and chemical processes in porous media result in nonequilibrium [e.g., *Rugner et al.*, 1999]. For a subset of solutes, a realistic model is [e.g., *Li and Brusseau*, 2000]:

$$\begin{aligned} &\frac{\partial}{\partial t}N = \kappa\,(K_d\,C - N) \quad \Rightarrow \\ &N(\mathbf{x}, t) = \kappa\,K_d \exp(-\kappa\,t)\int_0^t \mathrm{d}\tau \exp(\kappa\,\tau)\,C(\mathbf{x}, \tau), \end{aligned} \tag{4}$$

where $\kappa$ ($\mathrm{T}^{-1}$) and $K_d$ (–) are the desorption rate and linear equilibrium partitioning coefficient, respectively.

[11] At $t > 0$, a plume starts to migrate toward an accessible environment (hereafter termed as *control cylinder*) at a given radial distance $r$ from the injecting well (Figure 1). In practice, a CC consists of an array of wells/piezometers. We aim here to compute the solute flux $F$ across the lateral area of any CC. The procedure adopted herein follows that of *Dagan and Indelman* [1999]. Unlike these latter, the travel time Lagrangian approach is adapted to the radial flow configuration. More precisely, we consider the travel time $\tau$ of a fluid particle starting from a point $\mathbf{b}_0$ belonging to the well envelope of area $A_0$, and reaching the surface $A$ of the CC at $t = \tau$. As such, $\tau$ satisfies the Cauchy problem [*Dagan and Indelman*, 1999]

$$\frac{\mathrm{d}}{\mathrm{d}s}\tau = \frac{1}{V(s)}, \qquad \tau(0) = 0, \tag{5}$$

where $V(s) = \sqrt{\left(\frac{\mathrm{d}}{\mathrm{d}t}X_1\right)^2 + \left(\frac{\mathrm{d}}{\mathrm{d}t}X_2\right)^2 + \left(\frac{\mathrm{d}}{\mathrm{d}t}X_3\right)^2}$ is the modulus of the velocity along the curvilinear coordinate $s$ determined via the particle trajectory $\mathbf{X} = (X_1, X_2, X_3)$ solution of

$$\frac{\mathrm{d}}{\mathrm{d}t}\mathbf{X} = \mathbf{V}(\mathbf{X}), \qquad \mathbf{X}(0) = \mathbf{b}_0. \tag{6}$$

[12] Thus, the curve $s = s(\tau)$ represents the characteristic line for the fluid particle, and therefore along it one has $\frac{\partial}{\partial x_i} = \frac{1}{V_i(\mathbf{x})}\frac{\partial}{\partial \tau}$. As a consequence, along the curve $s = s(\tau)$ equation (3) can be written as

$$\frac{\partial}{\partial t}(C+N) + \frac{\partial}{\partial \tau}C = 0. \tag{7}$$

[13] It is seen that equation (7) represents the one-dimensional version of equation (3) (with unit velocity). The three-dimensional nature of the former problem stems from the dependence of $\tau$ upon the trajectory.

[14] We consider an injection mode that is proportional to the flux and denote by $\gamma(\tau, t)$ the solution of equation (7) corresponding to a Dirac pulse. The solute flux through the element $\mathrm{d}\mathbf{b} \in A$ is given by $\mathrm{d}F = \mathrm{d}\mathbf{b}\,n\,V_r\,\gamma(\tau, t) = \mathrm{d}\mathbf{b}_0\,n\,V_0\,\gamma(\tau, t)$, where the latter equality results from the fluid continuity equation ($q_r/n = V_r$ and $q_0/n = V_0$ represent the radial velocity through the CC and the well envelope, respectively). Thus, the solute flux at the CC reads as follows:

$$F(t; \mathbf{x}) = n\int_{A_0}\int_0^t \mathrm{d}\mathbf{b}_0\,\mathrm{d}t'\,C_0(t'; \mathbf{b}_0)\,V_0(\mathbf{b}_0; x_3)\,\gamma(\tau, t-t'), \tag{8}$$

where $C_0(t; \mathbf{b}_0)$ accounts for the solute injection mode through the well. Even if not explicitly reported on the right-hand side of equation (8), it is worth reminding that $F$ is clearly a function of the position $\mathbf{x}$ due to the dependence of the random field $\tau$ upon it. Similarly, the fluid flux $Q_f$ is given by

$$Q_f(x_3) = n\int_{A_0}\mathrm{d}\mathbf{b}_0\,V_0(\mathbf{b}_0; x_3). \tag{9}$$

[15] Since both $V_0$ and $\gamma$ are RSFs so are $F$ and $Q_f$. To compute their spatial averages $\overline{F}$ and $\overline{Q}_f$, we shall assume that the thickness $B$ of the aquifer is much larger than the vertical integral scale $I_v$ so that one can replace the spatial averages with the ensemble means (ergodic hypothesis), i.e.,

$$\overline{F}(t; \mathbf{x}) \simeq \langle F(t; \mathbf{x})\rangle = n\int_{A_0}\int_0^t d\mathbf{b}_0\,dt'\,C_0(t'; \mathbf{b}_0)\langle V_0(\mathbf{b}_0; x_3)\gamma(\tau, t-t')\rangle \tag{10}$$

$$\overline{Q}_f \simeq \langle Q_f(x_3)\rangle = n\langle V_0\rangle A_0. \tag{11}$$

[16] Note that equation (11) relies on the stationarity of $V_0$, being this latter proportional to the stationary RSF $Y$ [*Indelman and Dagan*, 2004]. To compute the quantity $\langle V_0\,\gamma(\tau, t)\rangle$, we take advantage of the relationship

$$g(\tau; \mathbf{x}) = \langle V_0\rangle^{-1}\int \mathrm{d}V_0\,V_0\,g(\tau, V_0; \mathbf{x}) \tag{12}$$

relating the joint probability density function (PDF) of $\tau$ and $V_0$ to that of the travel time. Since equation (12) slightly differs from the standard definition of marginal $g(\tau; \mathbf{x})$, it is worth deriving it in the sequel. Thus, we start

from the definition of conditional expectation $\langle V_0|\tau\rangle$ and use the stationarity of $V_0$ to have

$$\langle V_0|\tau\rangle = \int \mathrm{d}V_0\, V_0\, g(V_0|\tau;\mathbf{x}) = \langle V_0\rangle, \tag{13}$$

where $g(V_0|\tau;\mathbf{x})$ represents the conditional PDF of $V_0$. Multiplication of equation (13) by $g(\tau;\mathbf{x})$, and recalling the fundamental relationship between conditional and unconditional probabilities, i.e., $g(\tau, V_0;\mathbf{x}) = g(V_0|\tau;\mathbf{x})g(\tau;\mathbf{x})$, leads to (12).

[17] The relationship (12) simplifies the computation of $\langle V_0\,\gamma(\tau,t)\rangle$ as follows:

$$\begin{aligned}\langle V_0\,\gamma(\tau,t)\rangle &= \int_0^\infty \int \mathrm{d}\tau\,\mathrm{d}V_0\,\gamma(\tau,t)\,V_0\,g(\tau,V_0;\mathbf{x}) \\ &= \langle V_0\rangle \int_0^\infty \mathrm{d}\tau\,\gamma(\tau,t)\,g(\tau;\mathbf{x}).\end{aligned} \tag{14}$$

[18] Hence, the BTC $\overline{C}^f(t;\mathbf{x}) = \frac{\overline{F}(t;\mathbf{x})}{\overline{Q}_f}$ is obtained from equation (10) to (11) as

$$\begin{aligned}\overline{C}^f(t;\mathbf{x}) \simeq \frac{\langle F(t;\mathbf{x})\rangle}{\langle Q_f\rangle} = \frac{1}{A_0}\int_{A_0}\int_0^\infty \int_0^t \mathrm{d}\mathbf{b}_0\,\mathrm{d}\tau\,\mathrm{d}t'\,C_0(t';\mathbf{b}_0) \\ \gamma(\tau,t-t')\,g(\tau;\mathbf{x}).\end{aligned} \tag{15}$$

[19] Overall, $\overline{C}^f$ is expressed by means of a multiple quadrature whose physical meaning is straightforward: the BTC is sought as ensemble average along noninteracting (due to the neglect of pore-scale dispersion) flow paths where solute particles have (for given $t$) reached the CC. It is interesting to note that, while at flow-path scale the solute spreading is due to the reactive processes solely, the BTC will also be affected by the stochastic spreading due to the average upon the flow paths. For a conservative solute (i.e., $N \equiv 0$) one has $\gamma(\tau,t) = \delta(\tau - t)$, and equation (15) becomes

$$\overline{C}^f(t;\mathbf{x}) = \frac{1}{A_0}\int_{A_0}\int_0^t \mathrm{d}\mathbf{b}_0\,\mathrm{d}t'\,C_0(t';\mathbf{b}_0)\,g(t-t';\mathbf{x}). \tag{16}$$

[20] Our aim now consists in evaluating equation (15) given: (i) the reactive process (encompassed in the function $\gamma$), (ii) the function $C_0(t';\mathbf{b}_0)$, and (iii) the PDF $g(\tau;\mathbf{x})$. The crux of the matter consists in computing $g(\tau;\mathbf{x})$ as generated by the WF. This is still a difficult task, and some additional assumptions are needed to obtain a simple solution for the transport problem.

### 2.3. Simplifying Assumptions and Solution of the Flow Field

[21] An analytical solution of the flow field has been derived by *Indelman and Dagan* [1999] under some simplifying assumptions that are also adopted herein, and therefore it is worth recalling briefly.

[22] The well is replaced by a line of singularities at $r = 0$. This implies that to satisfy the boundary condition of given head along the well, the velocity $V_0$ must be proportional to the log conductivity $Y(0,0,x_3)$. Moreover, the condition (2) is incorporated into the flow equation (1) by adding a Dirac function. Hence, equation (1) is now replaced by

$$\nabla\cdot(K\nabla H) = -Q_w\frac{K}{\overline{K}}\delta(\mathbf{r}), \qquad \overline{K} = \frac{1}{B}\int_0^B \mathrm{d}x_3\,K(0,0,x_3). \tag{17}$$

This assumption leads to very accurate results when $r_w \ll I$. Since, generally, $r_w = \mathcal{O}(\mathrm{cm})$ and $I = \mathcal{O}(\mathrm{m})$, equation (17) can be used in most of the practical applications.

[23] We consider an unbounded domain, so that the vertical average and ensemble average can be interchanged, i.e., $\overline{K} \simeq \langle K\rangle$. This is admissible if $B \gg I_v$, a condition which is met in most of the real settings. In fact, one can assume $B \to \infty$ (or equivalently $\Omega \equiv \mathbb{R}^3$).

[24] A first-order approximation in $\sigma_Y^2$ (appropriate for mildly heterogeneous formations) is adopted to compute the fluctuation of the flux

$$\mathbf{q}^{(1)}(\mathbf{x}) = -K_A[Y'(\mathbf{x})\nabla H^{(0)}(\mathbf{x}) + \nabla H^{(1)}(\mathbf{x})] \qquad (Y' = Y - \langle Y\rangle), \tag{18}$$

being $H^{(0)}$ and $H^{(1)}$ the mean and fluctuation of the head, respectively. It has been shown [*Riva et al.*, 2006] that such an approximation leads to a robust (till to $\sigma_Y^2 \simeq 1$) estimate of the second-order moment of the travel time.

[25] We deal with anisotropic formations characterized by an anisotropy ratio $\lambda = \frac{I_v}{I} \le 0.2$. For these formations, it was found [*Indelman and Dagan*, 1999] that accurate solutions for transport are obtained by retaining only the first term of the right-hand side of equation (18). Since sedimentary formations [see, e.g., *Rubin* 2003, Tables 2.1 and 2.2] are as a rule strongly anisotropic (i.e., $\lambda \ll 1$), such an approximation is relevant for the applications.

[26] In summary, under the above-mentioned assumptions, the mean $\frac{q^{(0)}(r)}{n} = U(r)$ and radial fluctuation $u_r(\mathbf{x})$ of the velocity are given by

$$U(r) = \frac{K_A}{n}E^{(0)}(r), \qquad u_r(\mathbf{x}) \simeq U(r)\,Y'(\mathbf{x}), \qquad E^{(0)}(r) = \frac{Q_w}{2\pi K_A r}. \tag{19}$$

### 2.4. PDF of Travel Time

[27] Our approach relies on the fact that the probability $p$ that a fluid particle with given velocity $V_0$ has crossed the CC (at any radial distance $r$ from the well) is the same as the probability that the radial component $X_r$ of the particle trajectory is greater than $r$, i.e., $\mathrm{P}(\tau \le t) \equiv \mathrm{P}(X_r \ge r)$. In an equivalent manner, one can say that when $t > \tau$ the fluid particle is beyond the CC. Generally, such a distribution should be considered as the "first arrival" one to remark the fact that particles can also go back after crossing the CC (a comprehensive exposition on such a topic can be found by *Redner* [2001]). Thus, to avoid this occurrence that would lead to some shortcomings (especially with respect to the mass balance between the well and the CC),

one has to impose the extra condition of *absorbing barrier* at the CC. However, in our case, the assumption of moderate heterogeneity implies that the trajectory of any solute particle slightly differs from the mean trajectory (which is a straight line), and therefore solute particles do not go back after crossing the CC. That is why the first arrival and the travel time PDF are identical. For mathematical convenience, the PDF $g$ is expressed as function of the mean trajectory $R$ (for details, see Appendix A), the final result being

$$g(R;r) = \frac{Q_w}{2\pi n R}[\chi_r(R) + g_w(R;r)]\,\mathcal{N}_r[R, \overline{X}_{rr}(R)], \tag{20}$$

$$g_w(R;r) = \left\{\frac{\mathrm{d}}{\mathrm{d}R}\ln\left[\frac{\sigma_{X_r V_0}(R)}{\langle V_0\rangle}\right] - \frac{(R-r)\chi_r(R) + D_{rr}(R)}{X_{rr}(R)}\right\}\frac{\sigma_{X_r V_0}(R)}{\langle V_0\rangle}, \tag{21}$$

$$\chi_\rho(R) = 1 - (R-\rho)\frac{D_{rr}(R)}{X_{rr}(R)}, \qquad \mathcal{N}_\rho(m, s^2) = \frac{1}{\sqrt{2\pi}\,s}\exp\left[-\frac{(\rho-m)^2}{2s^2}\right], \tag{22}$$

$$D_{rr}(R) = \frac{1}{2}\frac{\mathrm{d}}{\mathrm{d}R}X_{rr}(R) = \frac{\sigma_Y^2}{3}\int_0^R \mathrm{d}\overline{r}\,\rho_Y(\overline{r}, 0)\left(1 - \frac{\overline{r}^3}{R^3}\right). \tag{23}$$

[28] The variance $X_{rr}$ (see equation (A8)) and the corresponding macrodispersion coefficient $D_{rr}$ are easily computed after specifying the shape of $\rho_Y$, i.e.,

$$\frac{X_{rr}(R)}{I^2} = \frac{2\,\sigma_Y^2}{3R^2}\begin{cases} \dfrac{R^2}{2}(2R-3) + 3[1-(1+R)\exp(-R)] & \text{(exponential)} \\ R^3\,\mathrm{erf}\left(\dfrac{\sqrt{\pi}}{2}R\right) + \dfrac{1}{\pi^2}\left[2(\pi R^2 - 2)\exp\left(-\pi\dfrac{R^2}{4}\right)\right. & \\ \quad \left. +4 - 3\pi R^2\right] & \text{(Gaussian)}, \end{cases} \tag{24}$$

and

$$\frac{D_{rr}(R)}{I} = \frac{\sigma_Y^2}{3R^3}\begin{cases} R^3 - 6 + 3\,(R^2 + 2R + 2)\exp(-R) & \text{(exponential)} \\ R^3\,\mathrm{erf}\left(\dfrac{\sqrt{\pi}}{2}R\right) + \dfrac{2}{\pi^2}\left[(\pi R^2 + 4)\right. & \\ \quad \left. \exp\left(-\pi\dfrac{R^2}{4}\right) - 4\right] & \text{(Gaussian)} \end{cases} \tag{25}$$

where $R$ is now scaled by $I$, although for simplicity we have retained the same notation. Similarly, one has from the last term of equation (A10)

$$\sigma_{X_r V_0}(R) = \frac{\sigma_Y^2}{R}\langle V_0\rangle\begin{cases} 1 - (1+R)\exp(-R) & \text{(exponential)} \\ \dfrac{2}{\pi}\left[1 - \exp\left(-\dfrac{\pi}{4}R^2\right)\right] & \text{(Gaussian)}. \end{cases} \tag{26}$$

[29] It is seen that in the far field $\sigma_{X_r V_0}$ reduces like $R^{-1}$ since it results:

$$\sigma_{X_r V_0}(R) \simeq \frac{\sigma_Y^2}{R}\langle V_0\rangle\begin{cases} 1 & \text{(exponential)} \\ \dfrac{2}{\pi} & \text{(Gaussian)} \end{cases} \qquad R \gg 1. \tag{27}$$

[30] Thus, the cross correlation between $X_r$ and $V_0$ decays very slowly with $R$, and this further underlines the fact that one has to deal with very large distances before regarding the travel time $\tau$ as a Gaussian random variable.

[31] In Figure 2, we have depicted the scaled PDF (continuous line) $\frac{n\pi I^2}{Q_w}\,g$ versus $\frac{R}{I}$ for $r = I$. For simplicity, we present results for exponential autocorrelation (the same conclusions are obtained for Gaussian $\rho_Y$). For comparison purposes, we have also shown (dotted line) the scaled PDF $\frac{I}{U_\infty}\,g^{(\mathrm{u})}$ pertaining to a MU flow (see Appendix B for details). Besides being important for understanding the evolution of reactive transport, these PDFs also represent the BTCs pertaining to a pulse of passive tracer, and therefore they enable one to appreciate the differences between transport in MU flows and transport in WF. To show the transition due to different degrees of the medium heterogeneity, we have depicted the PDFs for some values of $\sigma_Y^2$. When the hydraulic conductivity is certain ($\sigma_Y^2 = 0$), the PDFs degenerate (due to the neglect of pore-scale dispersion) into a Dirac distribution propagating on the front $R/I$.

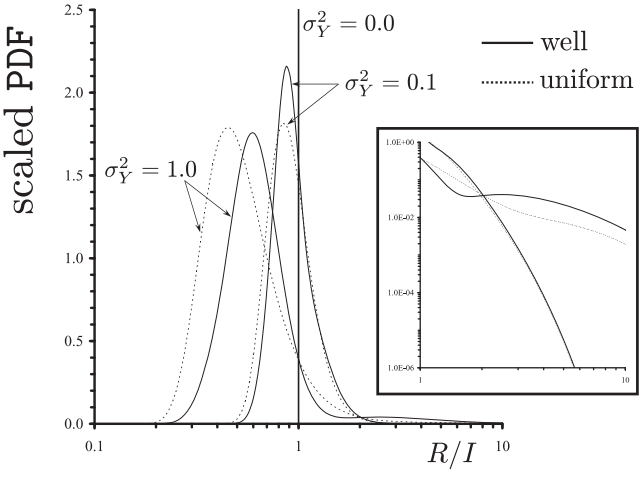


**Figure 2.** Scaled PDFs pertaining to a well (continuous line) and MU (dashed line) flow as function of $R/I$ for different $\sigma_Y^2$. Other parameter values: $r = I$ and $\lambda = 0.1$.

In this case, there is no difference between transport in WF and in MU one. Uncertainty in the hydraulic conductivity ($\sigma_Y^2 \neq 0$) smoothes PDFs, leading to asymmetric curves. The asymmetry increases with $\sigma_Y^2$. In particular, for higher $\sigma_Y^2$, tailing in the PDF is more persistent for the WF. This is explained by recalling that, unlike the MU flow, the radial velocity reduces like $R^{-1}$. Thus, tracer particles released with a relatively small velocity will take more time to reach a given CC as compared with those in a MU one. This kinematical picture also explains why the early arrivals in the WF are delayed as compared with those observed in a MU flow.

## 3. Discussion of Results

[32] We wish to illustrate the impact of linear nonequilibrium sorption/desorption (4) upon the BTCs. In particular, for high desorption ($\kappa \to \infty$), the sorbed and fluid concentrations mix instantaneously, and one recovers the linear equilibrium model, i.e.,

$$K_d\, C - N = \frac{1}{\kappa}\frac{\partial}{\partial t} N \simeq 0 \quad \Rightarrow \quad N \simeq K_d\, C. \tag{28}$$

[33] At the other extreme of zero mixing ($\kappa \to 0$), the sorbed phase is completely blocked off, and the solute behaves like a conservative one. The model (4) can also be used to mimic unidirectional solute transfer from the solid to the water phase (e.g., leaching from waste disposal sites) by setting $K_d = 0$. Thus, equation (4) represents a relatively general model for linear reactions that can incorporate both equilibrium and nonequilibrium processes. It is interesting to note that the effect of pore-scale dispersion (that is formally neglected) is indirectly accounted for via the kinematical mass transfer.

[34] The characteristic reaction function $\gamma$ for the model (4) has been derived by *Lassey* [1988]:

$$\gamma(\tau, t) = \exp(-\kappa K_d\, t)\delta(t-\tau) + K_d\, \kappa^2 \tau \exp[-\kappa\,(K_d\,\tau + t - \tau)] \tilde{\mathrm{I}}_1[K_d\, \kappa^2 \tau (t-\tau)]\chi(t-\tau) \tag{29}$$

with $\tilde{\mathrm{I}}_1(Z) \equiv \mathrm{I}_1(2\sqrt{Z})/\sqrt{Z}$, whereas $\mathrm{I}_1$ represents the modified Bessel function of the first kind of order one ($\chi$ is the Heaviside step function). It is seen that the $\gamma$-function is expressed as the superposition of: (i) a continuous distribution due to nonequilibrium effects and (ii) a propagating pulse which decays exponentially with $t$. The reaction function (29) can be further generalized to account for degradation in the fluid concentration. In this case, the Lagrangian equation (7) can be written as

$$\frac{\partial}{\partial t}\,(C_\mu + N_\mu) + \frac{\partial}{\partial \tau}\, C_\mu = -\mu\, C_\mu, \tag{30}$$

where $\mu$ ($\mathrm{T}^{-1}$) the (constant) degradation coefficient. The solution $C_\mu$ is obtained from that of equation (7) as $C_\mu(\tau, t) = \exp(-\mu\, t)\, C(\tau, t)$. Hence, the sorbed concentration $N_\mu$ is computed by replacing $C$ with $C_\mu$ into the second term of equation (4).

[35] For a pulse of constant strength $C_0 = \frac{M_0}{n\pi I^2}$ ($M_0$ is the injected mass per thickness), the BTC is computed from equation (15) as

$$\frac{\overline{C}^f(t'; r)}{C_0} = \frac{1}{2\sqrt{t'}}\, \exp(-\mathrm{Da}\, K_d\, t')\, g(\sqrt{t'}; r) + \frac{\mathrm{Da}}{2}\sqrt{K_d\, t'} \int_0^1 \mathrm{d}y\, g(\sqrt{y\, t'}; r)\, \Upsilon(y; \mathrm{Da}\, t') \tag{31}$$

$$\Upsilon(y; x) = \frac{\mathrm{I}_1[2\, x\sqrt{K_d\, y(1-y)}]}{\sqrt{1-y}}\, \exp[-x(K_d\, y + 1 - y)],$$

where Da is the Damköhler number defined as the ratio between the characteristic flow time $t_c = \frac{n\pi I^2}{Q_w}$ and the reaction rate $\kappa^{-1}$ ($t' = t/t_c$).

[36] In Figure 3, we have shown the BTC (equation (31)) versus $t'$ for some values of Da at $r = I$ ($K_d = 2$ and $\sigma_Y^2 = 0.5$). For a very slow reaction (Da $\to$ 0), the solute behaves conservatively, whereas for a fast reaction (Da $\to \infty$) the solute distribution is close to the equilibrium (with the partition coefficient $K_d$). At intermediate values of the Damköhler number, the BTC clearly exhibits a tail due to the delay caused by the ongoing solute transfer between the sorbed and liquid phases. This tail is confined between the BTC corresponding to Da $= K_d = 0$ (i.e., passive scalar) and the one corresponding to an equilibrium-dominated transport mechanism, i.e., Da $\to \infty$ (with $K_d \neq 0$). Accounting for solute degradation produces a further dumping in the BTCs.

### 3.1. Comparison With Experimental Data

[37] It is interesting to illustrate the application of our model to real data. Generally, there are very few forced tracer tests, and most lack the amount of data required for validation purposes (see discussion in *Gelhar et al.* [1992]). In fact, it is very difficult to obtain date under the various

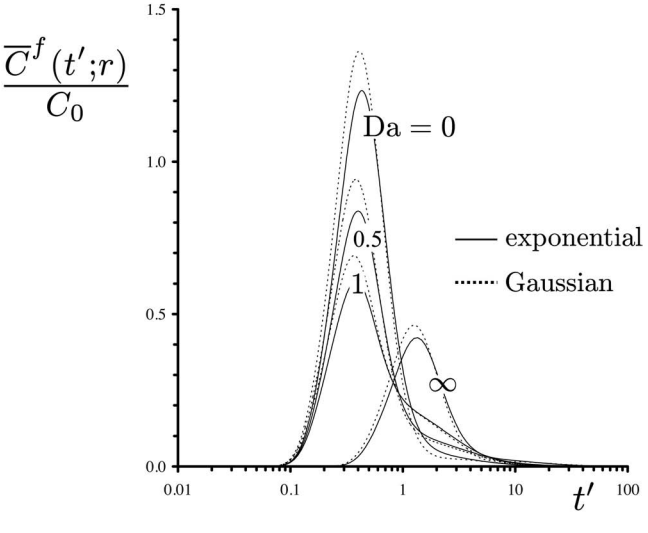


**Figure 3.** Normalized reactive BTC (31) versus the scaled time $t' = t/t_c$ at $r = I$ for different values of the Damköhler number Da. Other parameters: $\sigma_Y^2 = 0.5$ and $K_d = 2$.

flow regimes, fluctuations in the mean flow direction, nonuniformity of the flow, etc. Nevertheless, we found in the literature [*Fernandez-Garcia et al.*, 2004] a divergent flow tracer test (DFTT) suitable for comparison purposes. Although the test aquifer was artificially packed, it exhibits hydraulic properties resembling those found in some real settings [see *Gelhar et al.*, 1992; *Rubin*, 2003]. Thus, this experiment has the unusual advantage that the heterogeneity structure of the hydraulic conductivity is relatively well defined; therefore, reducing the uncertainty related to the estimate of the statistical parameters.

[38] The DFTT is described in detail by *Fernandez-Garcia et al.* [2004]. For the sake of completeness, the test (whose experimental setup is sketched in Figure 4) is described briefly herein. A sand tank (243.8 cm long, 121.9 cm wide, and 63.5 cm high) was constructed in the laboratory. The heterogeneity structure was artificially created by packing (for a complete description of the methodology, see *Chao et al.* [2000] and *Fernandez-Garcia et al.* [2004]) five different types of sands (the porosity $n$ was approximately 0.38). The final arrangement of sands packs was such that the conductivity is described by a geometric mean $K_G = \exp\langle Y\rangle = 116.7$ m d$^{-1}$ and standard deviation $\sigma_Y \simeq 1.3$. As for the statistical properties of the $Y$-random field, the autocorrelation was characterized by anisotropic structure with $I \simeq 10$ cm and $\lambda \simeq 0.2$.

[39] A fully penetrating well located at the center of the aquifer in conjunction with a peristaltic pump was used to force the flow at a constant volumetric rate (95 mL min$^{-1}$). After reaching steady-state conditions, a pulse of lithium bromide (LiBr) was added into the injecting well over a period of 5 min. Bromide concentrations with time were monitored by three batteries (each one formed by four piezometers) located at: (i) $r = 22$ cm (battery E), (ii) $r = 35$ cm (battery I), and (iii) $r = 45$ cm (battery K) from the well (Figure 4). Since bromide behaves as a passive scalar, the BTC is obtained by setting $\mathrm{Da} = K_d = 0$ into equation (31).

[40] The comparison between the analytical model (continuous line) and the experimental (discrete symbols) normalized BTCs $\overline{C}^f/C_0$ is shown in Figure 5. For the three relative distances ($r/I = 2.2$, 3.5, and 4.5), the BTCs were computed by averaging the four concentration curves monitored by the batteries E-I-K of piezometers. Before continuing, it is important to observe here that the geometrical

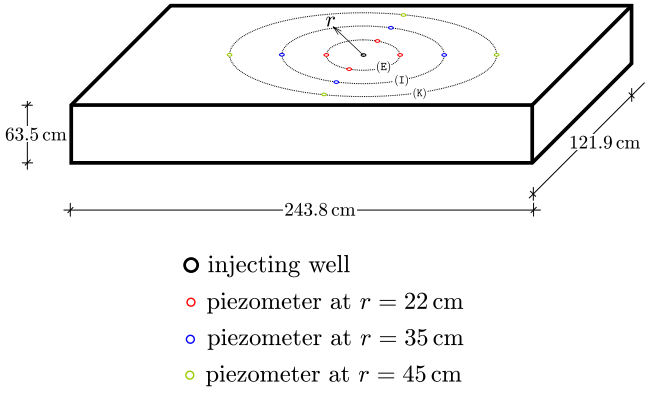


**Figure 4.** Three-dimensional view of the setup of *Fernandez-Garcia et al.* [2004].

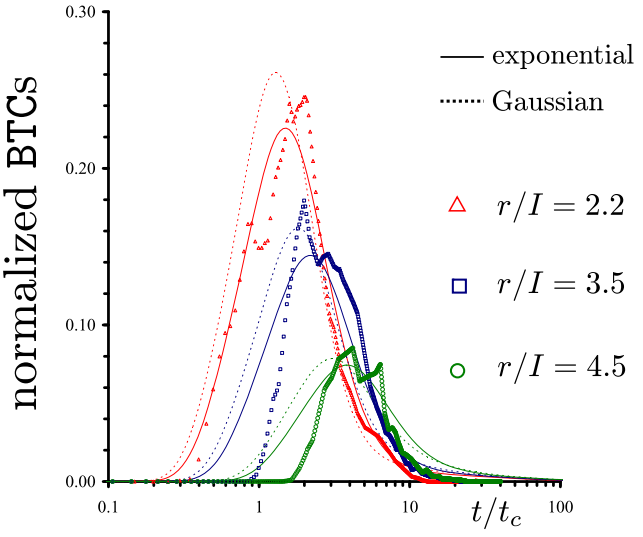


**Figure 5.** Comparison between theoretical (lines) and measured (symbols) normalized BTCs at three-scaled radial distances $r/I$.

configuration of the DFTT implies that $\lambda I/B = 2$ cm/63.5 cm $= 0.03$, and therefore transport can be regarded as ergodic. In addition, it should be noted that the value (i.e., $\sigma_Y \simeq 1.3$) of the standard deviation of $Y$ is slightly larger than one. However, as it will be immediately clear, this does not represent a strong limitation, also in view of the other sources of uncertainty (for instance, those related to the measuring devices).

[41] Generally, the model slightly underpredicts the position of the center of gravity $R = R(t')$. This small disagreement is mainly attributed to the uncertainty in the hydraulic properties. In fact, even if the artificial aquifer was packed to fit a given $Y$ distribution, it nevertheless exhibited some uncertainty in the resulting distribution of the log conductivity (see discussion in *Fernandez-Garcia et al.* [2004]). More important, the experimental BTCs were computed by averaging the concentration values at only four radial locations. In fact, even if ergodicity is ensured since from the beginning due to the fully sampling of the well (for details, see *Indelman and Dagan* [1999]), more sampling would have been desirable to fully detect the propagating plume. This experimental aspect (together with the fact that $\sigma_Y \simeq 1.3$) represents another reason to explain such a small disagreement. Finally, the proposed comparison also represents a quantitative way of testing the assumption (at least when computing the BTCs) of neglecting the pore-scale dispersion.

## 4. Concluding Remarks

[42] The problem investigated here is that of solute macrodispersion into a radial flow configuration. The plume spreads due to the velocity fluctuations that are caused by the spatial variability of the conductivity $K$. The difficulty of such a problem stems from the fact that, unlike the common natural gradient conditions, the flow pattern is nonuniform in mean. To reduce the mathematical complexity (while retaining the most relevant features of the problem at hand), a few simplifying assumptions have been adopted:

thick aquifer, fully penetrating well of steady discharge and stationary lognormal conductivity. By assuming weak heterogeneity and by dealing with highly anisotropic formations, we derive a simple solution to the transport problem.

[43] The main objective is to study transport of a reactive solute that is sorbed reversibly by the immobile phase (e.g., soil aggregates, stagnant zones, rock matrix) while being advected by the mobile (i.e., fluid) phase. By following *Cvetkovic and Dagan* [1994], the transport equation is rewritten in the one-dimensional domain $(\tau, t)$ along streamlines. Central to the present study is the PDF of $\tau$ which is derived consistently with the assumptions adopted herein. In particular, it is shown that the travel time $\tau$ can be regarded as a Gaussian variable only in the far field.

[44] The effect of sorption upon solute concentration in the mobile phase is manifested in the existence of a wake of solute trailing behind the propagating pulse. This wake, represented by the second term of equation (29), is confined to the stream tubes of the fluid flow (no mechanism of transverse exchange being present). At aquifer scale, the heterogeneity in the convective mechanism produces a further separation into parcels that move quicker than the mean through zones of higher permeability (for given distance $r$), with the opposite occurring in low-conductivity regions.

[45] Besides the theoretical interest, results of the present paper are also useful for practical applications. The model is tested against a forced-gradient experiment [*Fernandez-Garcia et al.*, 2004]. The good agreement with experimental data demonstrates that stochastic modeling is a valuable tool to grasp the transport outcome in forced-gradient tracer tests.

## Appendix A: PDF of the Travel Time in Radially Diverging Flows

[46] By following the procedure of *Cvetkovic and Dagan* [1996] and *Dagan* [1989], we derive an analytical expression for the PDF of the travel time $\tau$ consistent with the assumptions mentioned in section 2.4. Hence, with $f(X_r, V_0; t)$ as the joint PDF of $X_r$ and $V_0$ at time $t$, one has

$$\int_0^t \mathrm{d}\tau\, g(\tau, V_0; r) = G(t, V_0; r) = \int_r^\infty \mathrm{d}X_r f(X_r, V_0; t). \tag{A1}$$

[47] We are now in a position to compute the cumulative density function $G(\tau; r)$ of $\tau$. In fact, by accounting for equation (12), $G$ is written as

$$G(\tau; r) = \int_0^\tau \mathrm{d}\overline{\tau}\, g(\overline{\tau}; r) = \frac{1}{\langle V_0\rangle}\int_0^\tau \int \mathrm{d}\overline{\tau}\, \mathrm{d}V_0\, V_0\, g(\overline{\tau}, V_0; r). \tag{A2}$$

[48] Then, insertion of the last term of equation (A1) into (A2) leads to

$$G(\tau; r) = \frac{1}{\langle V_0\rangle}\int_r^\infty \int \mathrm{d}X_r\, \mathrm{d}V_0\, V_0 f(X_r, V_0; \tau). \tag{A3}$$

[49] It is now clear that to derive $G(\tau; r)$ (and consequently the PDF of $\tau$), one has to compute the joint PDF $f(X_r, V_0; \tau)$. To do this, we remind that the trajectory fluctuation $X_r' = X_r - \langle X_r\rangle$ is given by [*Indelman and Dagan*, 1999, equations (27)–(29)],

$$X_r'(R; x_3) = U(R)\int_0^R \mathrm{d}\overline{r}\, \frac{u_r(\overline{r}, x_3)}{U^2(\overline{r})}, \qquad R = \sqrt{\frac{Q_w \tau}{n\pi}} \tag{A4}$$

and that from the second term of (19) the fluctuation $V_0' = V_0 - \langle V_0\rangle$ is

$$V_0'(x_3) \simeq \langle V_0\rangle\, Y'(0, 0, x_3), \qquad \langle V_0\rangle \equiv \text{constant}. \tag{A5}$$

[50] Thus, at the $\sigma_Y^2$-order $X_r$ and $V_0$ can be regarded as a bivariate normal. As a consequence, their joint PDF $f(X_r, V_0; \tau)$ reads as

$$f(X_r, V_0; \tau) = \frac{1}{2\pi\sqrt{\Delta}} \exp\left(-\frac{1}{2\Delta}\mathbf{c}^{\mathrm{T}}\Sigma^{-1}\mathbf{c}\right), \qquad \mathbf{c} = \begin{pmatrix} X_r' \\ V_0' \end{pmatrix}, \tag{A6}$$

where $\Sigma$ is the variance-covariance matrix, i.e.,

$$\Sigma = \begin{bmatrix} X_{rr} & \sigma_{X_r V_0} \\ \sigma_{X_r V_0} & \sigma_{V_0}^2 \end{bmatrix} \qquad (\Delta = \det\Sigma). \tag{A7}$$

[51] The quantity $X_{rr}$ is the variance $\langle X_r'^2(R; x_3)\rangle$ along radii of the particle trajectory [*Indelman and Dagan*, 1999],

$$X_{rr}(R) = \frac{2}{3}\sigma_Y^2 R\int_0^R d\overline{r}\, \rho_Y(\overline{r}, 0)\left(1 - \frac{3\overline{r}}{2R} + \frac{\overline{r}^3}{2R^3}\right), \tag{A8}$$

whereas $\sigma_{X_r V_0}(R) \equiv \langle X_r'(R, x_3)\ V_0'(0, 0, x_3)\rangle$ and $\sigma_{V_0}^2$ represent the cross variance between the particle trajectory and the velocity at the well and the variance of $V_0$, respectively. Substitution of equation (A6) into (A3) gives (after carrying out the involved quadratures) the cumulative density function of $\tau$, i.e.,

$$G(\tau; r) = \frac{1}{2}\,\mathrm{erfc}\left[\frac{r - R}{\sqrt{2\,\overline{X}_{rr}(R)}}\right] + \frac{\sigma_{X_r V_0}(R)/\langle V_0\rangle}{\sqrt{2\,\overline{X}_{rr}(R)}} \exp\left[-\frac{(r - R)^2}{2\,\overline{X}_{rr}(R)}\right] \qquad (\pi X_{rr} \equiv \overline{X}_{rr}). \tag{A9}$$

[52] Note that the dependence of $G$ upon $\tau$ stems from the fact that $R$ is a monotone increasing function of the travel time (see the second term of equation (A4)). The cross-variance $\sigma_{X_r V_0}$ is readily computed by employing the definition and accounting for the first term of equation (A4) and (A5). The result is

$$\sigma_{X_r V_0}(R) = U(R)\int_0^R \frac{\mathrm{d}\overline{r}}{U^2(\overline{r})}\langle u_r(\overline{r}, x_3) V_0'(x_3)\rangle \Rightarrow \frac{\sigma_{X_r V_0}(R)}{\langle V_0\rangle} = \frac{\sigma_Y^2}{R}\int_0^R \mathrm{d}\overline{r}\,\overline{r}\,\rho_Y(\overline{r}, 0). \tag{A10}$$

[53] From the last term of equation (A10), it is easy to show that $\sigma_{X_r V_0}(\infty) = 0$ for any $\rho_Y$, due to the progressive reduction of the conditioning effect of $V_0$ upon the particle

trajectory $X_r$ as $R$ increases. As such, in the far field the cumulative density function (A9) is approximated by

$$G(\tau;r) \approx \frac{1}{2}\,\mathrm{erfc}\left[\frac{r-R}{\sqrt{2\,\overline{X}_{rr}(R)}}\right] = \frac{1}{2}\left\{1+\mathrm{erf}\left[\frac{R-r}{\sqrt{2\,\overline{X}_{rr}(R)}}\right]\right\}. \tag{A11}$$

[54] The far-field approximation equation (A11) of $G$ shows that $\tau$ can be regarded as a Gaussian variable only asymptotically. By employing the definition and the chain rule of derivation, i.e.,

$$g(\tau;r) = \frac{\partial}{\partial\tau}G(\tau;r) = \frac{\partial R}{\partial\tau}\frac{\partial}{\partial R}G(R;r) = \frac{Q_w}{2n\pi R}\frac{\partial}{\partial R}G(R;r) \equiv g(R;r) \tag{A12}$$

leads to (20).

## Appendix B: PDF of the Travel Time in Mean Uniform Flows

[55] In this case, $g^{(\mathrm{u})}$ represents the PDF of the travel time of a fluid particle starting from the injection plane at $x_1 = 0$ and reaching any *control plane* at $x_1 > 0$. At $\sigma_Y^2$-order, $g^{(\mathrm{u})}$ has been derived by *Cvetkovic and Dagan* [1996] as a function of the variance $X^{(\mathrm{u})}(\overline{R})$ of the fluid particle trajectory, and the macrodispersion coefficient $D^{(\mathrm{u})}(\overline{R}) = \frac{1}{2}\frac{\mathrm{d}}{\mathrm{d}\overline{R}}X^{(\mathrm{u})}(\overline{R})$ (with $\overline{R} = \tau U_\infty$). The final result can be written as:

$$g^{(\mathrm{u})}(\overline{R};x_1) = U_\infty\sqrt{X^{(\mathrm{u})}(\overline{R})}\,g_0(\overline{R};x_1)\,\mathcal{N}_{x_1}(\overline{R},X^{(\mathrm{u})}) \tag{B1}$$

$$g_0(\overline{R};x_1) = \frac{\mathrm{d}}{\mathrm{d}\overline{R}}\left[\frac{D^{(\mathrm{u})}(\overline{R})}{\sqrt{X^{(\mathrm{u})}(\overline{R})}}\right] + \chi_{x_1}(\overline{R})\,\frac{\mathrm{d}}{\mathrm{d}\overline{R}}\left[\frac{\overline{R}-x_1}{\sqrt{X^{(\mathrm{u})}(\overline{R})}}\right], \tag{B2}$$

where the function $\chi_{x_1}$ is obtained from the first term of equation (22) after replacing $X_{rr}$ and $D_{rr}$ with $X^{(\mathrm{u})}$ and $D^{(\mathrm{u})}$, respectively. Here, we compute $X^{(\mathrm{u})}$ (and therefore $g^{(\mathrm{u})}$) in accordance with the assumptions recalled in this paper. This leads to

$$\frac{X^{(\mathrm{u})}(R)}{(I\sigma_Y)^2} = \int_0^R\int_0^R\int\frac{\mathrm{d}R'\mathrm{d}R''\mathrm{d}\mathbf{k}}{(2\pi)^{3/2}}\Phi(\mathbf{k})\exp[-\imath k_1(R'-R'')], \qquad R = \frac{\overline{R}}{I} \tag{B3}$$

being $\Phi(\mathbf{k}) = \int\frac{\mathrm{d}\mathbf{x}}{(2\pi)^{3/2}}\rho_Y(\mathbf{x})\exp(\imath\mathbf{k}\cdot\mathbf{x})$ the spectrum (i.e., Fourier transform of $\rho_Y$). Closed analytical expressions are obtained for specific shape of $\Phi$, i.e.,

$$\frac{X^{(\mathrm{u})}(R)}{(I\sigma_Y)^2} = 2\begin{cases} R+\exp(-R)-1 & \text{(exponential)} \\ R\,\mathrm{erf}\left(\frac{\sqrt{\pi}}{2}R\right) - \frac{2}{\pi}\left[1-\exp\left(-\frac{\pi}{4}R^2\right)\right] & \text{(Gaussian)}, \end{cases} \tag{B4}$$

and concurrently

$$\frac{D^{(\mathrm{u})}(R)}{I\sigma_Y^2} = \begin{cases} 1-\exp(-R) & \text{(exponential)} \\ \mathrm{erf}\left(\frac{\sqrt{\pi}}{2}R\right) & \text{(Gaussian)}. \end{cases} \tag{B5}$$

[56] It is interesting to observe that the first term of equation (B4) coincides with the approximation provided by *Dagan and Cvetkovic* [1993], i.e.,

$$\frac{X^{(\mathrm{u})}(R)}{(I\sigma_Y)^2} \simeq f(R;\lambda), \qquad f(R;\lambda) = \frac{2}{\xi(\lambda)}\{\xi(\lambda)R + \exp[-\xi(\lambda)R] - 1\} \tag{B6}$$

$$\xi(\lambda) = 1 + \frac{\lambda}{16(1-\lambda^2)^2}\left[(19-10\lambda^2)\lambda - (13-4\lambda^2)\,\frac{\arcsin\sqrt{1-\lambda^2}}{\sqrt{1-\lambda^2}}\right] \tag{B7}$$

in the limit $\xi(0) = 1$. Thus, although equation (B6) was derived on the basis of the computational efficiency [see *Severino et al.*, 2005], it becomes an exact $\sigma_Y^2$ -order result for stratified formations.

[57] **Acknowledgments.** The authors are deeply indebted to Daniel Fernàndez-Garcia (Polytechnic University of Valencia, Spain), Tissa H. Illangasekare (Colorado School of Mines, USA), and the U.S. Army Research Office for providing the complete data set concerning the DFTT. We are very grateful to the three anonymous reviewers for their thorough and helpful comments that significantly improved the earlier version of the manuscript. This research was partially supported by the Italian Ministry of University and Research under the PRIN 2008: Project Optimization Methods and Software for Inverse Problems (2008T5KA4L) and by the fund Solute Transport in Heterogeneous Media: Modeling and Computational Aspects. We also thank the Institute of Geophysics and Planetary Physics at Los Alamos National Laboratory for providing funding for this work.

## References

Andricevic, R., and V. Cvetkovic (1997), Relative dispersion for solute flux in aquifers, *J. Fluid Mech.*, *361*, 145–174.

Chao, C.-H., H. Rajaram, and T. H. Illangasekare (2000), Intermediate scale experiments and numerical simulations of transport under radial flow in a two-dimensional heterogeneous porous medium, *Water Resour. Res.*, *36*(10), 2869–2884, doi:10.1029/2000WR900096.

Chen, C. S. (1987), Analytical solution for radial dispersion with cauchy boundary at injection well, *Water Resour. Res.*, *23*(7), 1217–1224, doi:10.1029/WR023i007p01217.

Cvetkovic, V., and G. Dagan (1994), Transport of kinetically sorbing solute by steady random velocity in heterogeneous porous formations, *J. Fluid Mech.*, *265*, 189–215.

Cvetkovic, V., and G. Dagan (1996), Reactive transport and immiscible flow in geological media. II. Applications, *Proc. R. Soc. Lond. A*, *452*, 303–328.

Cvetkovic, V., G. Dagan, and H. Cheng (1998), Contaminant transport in aquifers with spatially variable hydraulic and sorption properties, *Proc. R. Soc. Lond. A*, *454*, 2173–2207.

Dagan, G. (1986), Statistical theory of groundwater flow and transport: Pore to laboratory, laboratory to formation, formation to regional scale, *Water Resour. Res.*, *22*(09S), 120S–134S, doi:10.1029/WR022i09Sp120S.

Dagan, G. (1989), *Flow and Transport in Porous Formation*, Springer, New York.

Dagan, G., and V. Cvetkovic (1993), Spatial moments of kinetically sorbing solute plume in a heterogeneous aquifer, *Water Resour. Res.*, *29*(12), 4053–4061, doi:10.1029/93WR02299.

Dagan, G., and P. Indelman (1999), Reactive solute transport in flow between a recharging and a pumping well in a heterogeneous aquifer, *Water Resour. Res.*, *35*(12), 3639–3647, doi:10.1029/1999WR900214.

Dagan, G., V. Cvetkovic, and A. Shapiro (1992), A solute flux approach to transport in heterogeneous formations: 1. The general framework, *Water Resour. Res.*, *28*(5), 1369–1376, doi:10.1029/91WR03086.

Fernandez-Garcia, D., T. H. Illagasekare, and H. Rajaram (2004), Conservative and sorptive forced-gradient and uniform flow tracer tests in three-dimensional laboratory test aquifer, *Water Resour. Res.*, *40*, W10103, doi:10.1029/2004WR003112.

Fiori, A., P. Indelman, and G. Dagan (1998), Correlation structure of flow variables for steady flow toward a well with application to highly anisotropic heterogeneous formations, *Water Resour. Res.*, *34*(4), 699–708, doi:10.1029/97WR02491.

Gelhar, L. W., C. Welty, and K. Rehfeldt (1992), A critical review of data on field-scale dispersion aquifer, *Water Resour. Res.*, *28*(7), 1955–1974, doi:10.1029/92WR00607.

Guadagnini, A., M. Berglund, and S. P. Neuman (2003), Three-dimensional steady state flow to a well in a randomly heterogeneous bounded aquifer, *Water Resour. Res.*, *39*(3), 1048, doi:10.1029/2002WR001443.

Hsieh, P. A. (1986), A new formula for the analytical solution of the radial dispersion problem, *Water Resour. Res.*, *22*(11), 1597–1605, doi:10.1029/WR022i011p01597.

Indelman, P., and G. Dagan (1999), Solute transport in divergent radial flow through heterogeneous porous media, *J. Fluid Mech.*, *384*, 159–182.

Indelman, P., and G. Dagan (2004), A note on well boundary condition for flow through heterogeneous formations, *Water Resour. Res.*, *40*, W03601, doi:10.1029/2003WR002602.

Indelman, P., A. Fiori, and G. Dagan (1996), Steady flow toward wells in heterogeneous formations: Mean head and equivalent conductivity, *Water Resour. Res.*, *32*(7), 1975–1983, doi:10.1029/96WR00990.

Indelman, P., S. C. Lessoff, and G. Dagan (2006), Analytical solution to transport in three-dimensional heterogeneous well capture zones, *J. Contam. Hydrol.*, *87*, 1–21, doi:10.1016/j.jconhyd.2006.04.005.

Lassey, K. R. (1988), Unidimensional solute transport incorporating equilibrium and rate-limited isotherms with first-order loss: 1. Model conceptualizations and analytical solutions, *Water Resour. Res.*, *24*(3), 343–350, doi:10.1029/WR024i003p00343.

Lessoff, S. C., and P. Indelman (2004), Stochastic determination of three-dimensional capture zones for a fully penetrating well, *Water Resour. Res.*, *40*, W03508, doi:10.1029/2003WR002703.

Li, Z., and M. L. Brusseau (2000), Nonideal transport of reactive solutes in heterogeneous porous media: 6. Microscopic and macroscopic approaches for incorporating heterogeneous rate-limited mass transfer, *Water Resour. Res.*, *36*(10), 2853–2867, doi:10.1029/2000WR900089.

Ptak, T., M. Piepenbrink, and E. Martac (2004), Tracer tests for the investigations of heterogeneous porous media and stochastic modelling of flow and transport: A review of some recent developments, *J. Hydrol.*, *294*, 122–163, doi:10.1016/j.jhydrol.2004.01.020.

Redner, S. (2001), *A Guide to First-Passage Processes*, Cambridge Univ. Press, Cambridge.

Riva, M., X. Sanchez-Vila, A. Guadagnini, M. D. Simoni, and M. Willmann (2006), Travel time and trajectory moments of conservative solutes in two-dimensional convergent flows, *J. Contam. Hydrol.*, *82*, 23–43, doi:10.1016/j.jconhyd.2005.06.014.

Rubin, Y. (2003), *Applied Stochastic Hydrogeology*, Oxford Univ. Press, New York.

Rugner, H., S. Kleineidamm, and P. Grathwohl (1999), Long term sorption kinetics of phenanthrene in aquifer materials, *Environ. Sci. Technol.*, *33*(10), 1645–1651.

Sanchez-Vila, X., and Y. Rubin (2003), Travel time moments for sorbing solutes in heterogeneous domains under nonuniform flow conditions, *Water Resour. Res.*, *39*(4), 1086, doi:10.1029/2002WR001399.

Severino, G., V. Cvetkovic, and A. Coppola (2005), On the velocity covariance for steady flows in heterogeneous porous formations and its application to contaminants transport, *Comput. Geosci.*, *9*, 155–177.

Severino, G., A. Santini, and A. Sommella (2008), Steady flows driven by sources of random strength in heterogeneous aquifers with application to partially penetrating wells, *Stoch. Environ. Res. Risk Assess.*, *22*, 567–582, doi:10.1007/s00477-007-0175-5.

Severino, G., A. Santini, and A. Sommella (2011), Macrodispersion by diverging radial flows in randomly heterogeneous porous media, *J. Contam. Hydrol.*, *123*, 40–49, doi:10.1016/j.jconhyd.2010.12.005.

Severino, G., D. M. Tartakovsky, G. Srinivasan, and H. Viswanathan (2012), Lagrangian models of reactive transport in heterogeneous porous media with uncertain properties, *Proc. R. Soc. Lond. A*, *468*, 1154–1174, doi:10.1098/rspa.2011.0375.

Valocchi, A. (1986), Effect of radial flow on deviation from local equilibrium during sorbing solute transport through homogeneous soils, *Water Resour. Res.*, *22*(12), 1693–1701, doi:10.1029/WR022i012p01693.